IEEE Access
Multidisciplinary | Rapid Review | Open Access Journal

Date of publication xxxx 00, 0000, date of current version xxxx 00, 0000.

*Digital Object Identifier 10.1109/ACCESS.2019.Doi Number*

# Collision Avoidance Planning Method of USV Based on Improved Ant Colony Optimization Algorithm (March 2019)

**First Hongjian Wang[1,*], Second Feng Guo[2], Third Hongfei Yao[3], Fourth Shanshan He[4], and Fifth Xin Xu[5]**

[1] College of Automation, Harbin Engineering University, Harbin, HLJ 150001 CHN
[2] College of Automation, Harbin Engineering University, Harbin, HLJ 150001 CHN
[3] College of Automation, Harbin Engineering University, Harbin, HLJ 150001 CHN
[4] College of Automation, Harbin Engineering University, Harbin, HLJ 150001 CHN
[5] College of Automation, Harbin Engineering University, Harbin, HLJ 150001 CHN

Corresponding author: First Hongjian Wang (e-mail: cctime99@163.com).

This work was supported in part by the National Natural Science Foundation of China (No. 61633008, No.51609046), and the Natural Science Foundation of Heilongjiang Province under Grant F2015035.

**ABSTRACT** In order to solve the problem of insufficient search ability of the unmanned surface vehicle (USV) collision avoidance planning algorithm, this paper proposes an improved ant colony optimization algorithm (ACO). Firstly, aiming at the static unknown environment, in order to improve the real-time performance of USV online planning, and considering the environmental characteristics of USV operation for improving ACO to search for the optimal path, a dynamic viewable method is proposed for the local environment model. Secondly, according to the known dynamic environment, based on the motion velocity model and International Regulations for Preventing Collisions at Sea (COLREGS), a reverse eccentric expansion method is designed to deal with the dynamic obstacles. Then, aiming at the problem that ACO has a slow convergence speed, an improved pseudo-random proportional rule is proposed to select the ant state transition. And the wolf pack allocation principle and the maximum-minimum ant system are used to update the global pheromone to avoid the search falling into local optimum. Finally, the convergence, real-time performance and stability of the improved ACO are verified through the simulation experiment of USV collision avoidance in the static unknown and dynamic known environment.

**INDEX TERMS** Unmanned surface vehicle (USV), ant colony optimization algorithm (ACO), viewable method, reverse eccentric expansion method, collision avoidance planning

## I. INTRODUCTION

As an autonomous marine vehicle, unmanned surface vehicle (USV) attracts wide attention due to its fast sailing speed, small ship scale and high intelligence. Its advantage lies in its ability to carry out dangerous and unsuitable tasks for manned vessels [1]. Therefore, it has broad development prospects in both military and civilian fields, and has become a research hotspot of intelligent equipment at home and abroad. Literatures [2][3] summarize the development history, research status and future trends of USV. At present, a variety of USVs have been applied in military and scientific research fields.

Collision avoidance planning is an important research direction in the development trend of USV. Its purpose is to find an optimal path without collision from the starting point to the target point in an unknown environment with obstacles [4]. It is both a prerequisite for the USV to complete its mission and an important indicator of the level of intelligence. At present, scholars from various countries have done a lot of research work on the USV collision avoidance planning method. Svec et al. have proposed a USV collision avoidance

This article has been accepted for publication in a future issue of this journal, but has not been fully edited. Content may change prior to final publication. Citation information: DOI 10.1109/ACCESS.2019.2907783, IEEE Access



method based on three path planning methods (A* algorithm, local boundary method and game tree method). The method combines the heuristic A* algorithm with the local boundary optimal programming, and obtains the obstacle information by using the game tree search method, so that the optimal path of the USV collision avoidance planning can be quickly obtained [5]. Liu et al. firstly, have rasterized the environment and established an environmental potential field based on distance factors. Finally, the fast step method is used to enable the formation USV to quickly plan the path in a complex, high sea state environment [6]. Kim et al. have combined Line-of-sight (LOS) navigation strategy and based on angular rate limitation (ARL) studied individual USV collision avoidance planning problems under high-speed motion conditions. Although this method is similar to the A* algorithm, ARL limits the convergence angle of LOS and considers the USV's own motion ability, the choice of planning points is different [7]. Based on International Regulations for Preventing Collisions at Sea (COLREGS), Tam et al. based on the encounter situation of the two ships and the evolutionary algorithm have achieved dynamic collision avoidance of the two ships. The method evaluates the feasibility of the USV collision avoidance plan in accordance with COLREGS based on the collision risk of obstacles at fixed time intervals [8][9]. For the purpose of USV navigation cost reduction, Song et al. have proposed a novel multi-layer fast stepping method (MFM), which firstly constructed an environment containing ocean current information, and established force field through attraction and repulsive force set in the environment. Finally, real-time collision avoidance of individual USV was realized based on the fast stepping method [10]. Due to the complex constraints, more uncertain factors and critical real-time demand of path planning for USV, an approach of fast path planning based on voronoi diagram and improved Genetic Algorithm has been proposed by Song et al., which makes use of the principle of hierarchical path planning. Simulation results verify that the optimal time is greatly reduced and path planning based on voronoi diagram and the improved Genetic Algorithm is more favorable in the real-time operation. [11].

The ant colony optimization algorithm (ACO) [12][13] was first proposed by the Italian scholar M. Dorigo and others. It is inspired by the behavior of simulating ant social division and collaborative learning. ACO has the advantages of positive feedback, parallelism and strong robustness, and has successful cases in solving path planning [14][15] and function optimization [16][17]. Aiming at the problem that ACO has a slow convergence speed and is easy to fall into the local optimum [18][19], many scholars at home and abroad have made many improvements. T. Stutzle et al. have proposed a Max-Min Ant System (MMAS) ACO to prevent premature convergence. However, when the average distribution of environmental information is in all directions, the pheromone released by the ant will mislead the decision behavior of the ant colony [20]. In order to solve the convergence speed problem of ACO, Yao et al. have proposed a heterogeneous feature ACO in robot path planning problem. By introducing the force field factor, the ant is driven to optimize the path to a higher fitness space, which effectively improves the search speed of the algorithm [21]. Cekmez et al. have proposed a multi-group cooperative optimization ACO to exchange optimal information to achieve data fusion, avoiding the algorithm falling into premature convergence [22]. I. Chaari et al. have proposed a new efficient hybrid ACO-GA method, using the ACO method to find the suboptimal solution, and then using the GA to search for the optimal solution in the suboptimal solution, which is used to solve the global robot path planning in static environment [23]. To enhance the global searchability and convergence speed of ACO, Cao has proposed an improved ACO and applied it to solve the robot global path planning problem. In the improved ACO, pheromone quantity is reinforced in some short paths of each cycle, and the pheromone evaporation rate is adjusted dynamically with the change of iterations [24].

Aiming at the problem of USV collision avoidance planning, firstly, in view of the static unknown environment, in order to improve the real-time performance of USV online planning, this paper combines the dynamic environment modeling method [25] with the improved ant colony optimization algorithm (IACO), and uses viewable method [26] to construct the local static unknown USV operation environment model. Secondly, in view of the known dynamic environment, based on the motion velocity model and COLREGS, the reverse eccentric expansion method is adopted to treat the dynamic obstacles. In addition, in order to improve the convergence speed of ACO and avoid falling into the local optimum, the improved pseudo-random proportion rule is adopted as the state transition rule, and the pheromone is updated globally by referring to the wolf pack allocation principle [27] and MMAS. Finally, IACO is used to realize the USV collision avoidance planning and to complete the simulation verification.

## II. ENVIRONMENTAL MODEL

### A. STATIC ENVIRONMENT MODEL

#### 1) USV COLLISION AVOIDANCE PLANNING STRATEGY

The dynamic environment modeling method adopted in this paper is to set up an environment window moving together with the USV under the condition of high-speed motion, and conduct a dynamic collision avoidance planning for the USV at a fixed time. In collision avoidance planning, only obstacles in the current rolling window are modeled. In this way, as the environment window keeps rolling forward, the optimization of USV online planning is greatly improved. Among them, the smaller the environment window design is, the less the environment information will be, and the faster the real-time planning speed will be. The larger the

This article has been accepted for publication in a future issue of this journal, but has not been fully edited. Content may change prior to final publication. Citation information: DOI 10.1109/ACCESS.2019.2907783, IEEE Access



environment window is, the greater the amount of information will be grasped. Because of the limited sensing range of the sensor carried by USV itself, USV in this paper adopts the analog environment sensing sensor (navigation radar) to obtain the static unknown environment, the size of the rolling window is set as the actual detection range of the navigation radar.

For the collision avoidance planning of static unknown obstacles, the dynamic environment modeling method designed in this paper has the following two characteristics:

- For each collision avoidance planning, all known obstacle information are included in the collision avoidance planning instead of only aiming at the environmental information in the rolling window. For static obstacles in the unknown environment, the collision avoidance planning always takes the end point as the target point.

In this paper, all static obstacles detected by USV sensors are stored in the obstacle information link list. Each collision avoidance planning will carry out global path planning based on all environmental information in the obstacle information link list. Although this will lead to more and more environmental information participating in dynamic programming, it also adds the "memory" function to the algorithm to avoid the USV falling into the local optimum and causing the USV to oscillate in the trap.

- Collision avoidance planning adopts new trigger mechanism of unknown environment information instead of fixed time interval.

In the course of navigation, if it encounters an environment that is not in the obstacle information list, it will add the environmental information to the obstacle information list, shorten the fixed time interval of the trigger, and increase the number of triggering plans. So not only can the newly discovered unknown obstacles respond quickly and effectively, and avoid unnecessary waste of triggering collision avoidance planning too frequently. In the absence of new environmental information, even if the planning is triggered multiple times, the USV navigation path will not change significantly.

In summary, when USV is performing local collision avoidance planning, each step of the environmental window scrolling must judge whether the USV navigation path is based on the known environmental information to collide with the unknown obstacle detected by the navigation radar. If there is no collision, USV continues to sail according to the originally planned path. Otherwise, the local environment will be modeled according to the navigation radar to obtain new unknown environment information, so as to find the local optimal path for the local collision avoidance planning of USV. Then USV will be sailed along the new path until it reaches the end of the route.

### 2) STATIC ENVIRONMENT MODELING METHOD

In this paper, USV uses analog navigation radar to obtain a static unknown environment. Navigation radar detects the surrounding environment by emitting electromagnetic waves and receiving the reflected waves from obstacles, that is, the intersection of electromagnetic waves and the surface of obstacles is the reflection point or obstacle point. As shown in figure 1, according to the distance $d_i$ and angle $\theta_i$ between each reflection point and the navigation radar, the position information of each obstacle vertex relative to the navigation radar is known, and the position information is converted into the position information relative to the center of mass of USV, so as to complete the detection of the local static unknown environment in the USV dynamic rolling window.

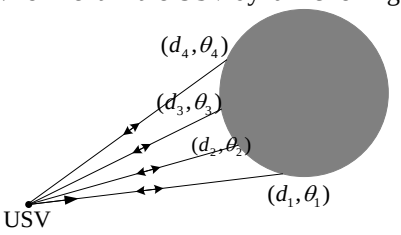


**FIGURE 1. Detection of unknown obstacles by navigation radar**

In order to facilitate ACO to search for the optimal path, this paper adopts viewable method to model the local static unknown environment in the dynamic rolling window. In view of the fact that the USV should be regarded as a particle in the collision avoidance planning, and that the actual USV has a specific size, the obstacles in the environment need to be expanded outwards equivalent. Where, this process is called expansion process [28], and the purpose of expansion is to improve the safety of the USV in the collision avoidance planning path.

a. Viewable inflation method

For the elliptical obstacle, according to the actual need to set the safe distance, it is expanded into an ellipse with the same ellipse center and a longer radius (longer radius refers to the safe distance), so that the Pythagorean theorem can be used to obtain the expanded ellipse external rectangle.

For polygonal obstacles, they are generally divided into convex polygonal and concave polygonal obstacles. In literature [29], the concave polygonal obstacles are expanded by the expansion method of convex polygonal obstacles, as shown in figure 2 (a), it can be seen that this way of inflation may lose the optimal path in the planning of collision avoidance, so this paper will design a applies to both the expansion method of the convex polygonal and concave polygonal obstacle, as shown in figure 2 (b).

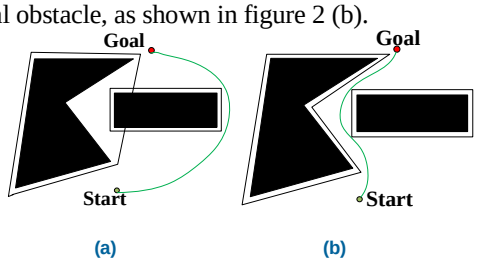


**FIGURE 2. (a)Puffing method 1, (b)Puffing method 2**

Therefore, this paper firstly uses the vector area method to determine whether the vertex of a polygon is convex or

This article has been accepted for publication in a future issue of this journal, but has not been fully edited. Content may change prior to final publication. Citation information: DOI 10.1109/ACCESS.2019.2907783, IEEE Access



concave. As shown in figure 3, polygons are set to form vectors in clockwise order. The area of the polygon is shown in formula (1) :

$$S_{ABCDEFG} = S_{ABba} + S_{BCcb} + S_{DEed} - S_{CDdc} - S_{EFfe} - S_{GFfg} - S_{AGga} \quad (1)$$

Where it takes the trapezoid area formula as an example, $x_i$ and $y_i$ are the coordinates of point $i$ , each trapezoid area is calculated according to formula (2). Obviously, when the direction of each vector of the polygon is as shown in figure 3, the sum obtained is positive.

$$S_{ABba} = \frac{1}{2}(y_A + y_B)(x_B - x_A) \quad (2)$$

If the vertex of a polygon is a concave point, the area of the vector triangle formed by the vertex and the neighboring point with the same vector direction as the polygon is opposite to the area of the vector polygon, for example $S_{ABCDEFG} \times S_{CDE} < 0$ . If the vertex of a polygon is a convex point, the area of the vector triangle formed by the vertex and the neighboring point with the same vector direction as the polygon is the same as the area of the vector polygon, for example $S_{ABCDEFG} \times S_{BCD} > 0$ .

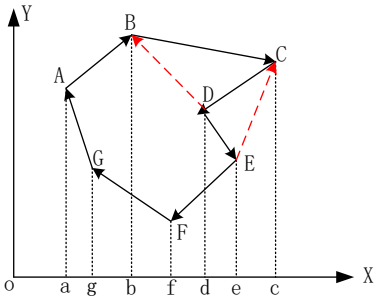


FIGURE 3. Vector area method

Secondly, according to the concavity and convexity of polygon vertex, the corresponding vertex expansion method is designed. As shown in figure 4 (a), vertex $A$ of the polygon is a convex point, and $A$ is used as the origin of the coordinate to establish a rectangular coordinate system. According to its neighboring points $F$ and $B$ , the angle between its angle bisector and the positive direction of the axis can be obtained, as shown in formula (3) :

$$\alpha = \angle FAX - \frac{\angle BAF}{2} \quad (3)$$

Where $h$ is the manually set safe distance, then the puffed obtained point is the intersection point between the reverse extension line of $\angle BAF$ angle bisector and the parallel line outside the polygon ABCDE with a distance of $h$ from $AB$ (or $AF$ ), as shown in formula (4) :

$$x = \frac{-h}{\left(\frac{y_B}{x_B} + \tan\alpha\right) \cdot \cos\left(\arctan\frac{y_B}{x_B}\right)}$$
$$y = \frac{\tan\alpha \cdot h}{\left(\frac{y_B}{x_B} + \tan\alpha\right) \cdot \cos\left(\arctan\frac{y_B}{x_B}\right)} \quad (4)$$

Similarly, as shown in figure 4 (b), the vertex $F$ of the polygon is a concave point, which can also be obtained by the above method. However, the obtained puffed point becomes the intersection point of $\angle AFE$ angular bisector and parallel lines outside the polygon $ABCDE$ and separated from $AF$ (or $FE$ ) by $h$ , instead of the reverse extension line of angular bisector.

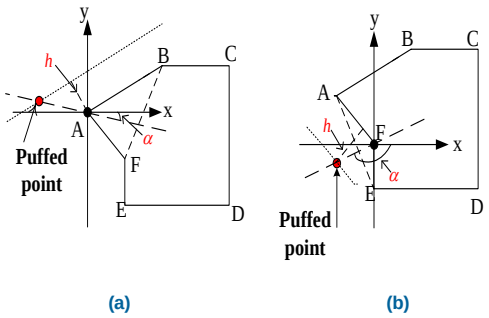


FIGURE 4. (a)Convex case, (b)Concave case

b. Viewable build method

The state transition point in IACO is the viewable point in the viewable view, so the key to view construction is to judge the visibility of any two visible points. The so-called visibility refers to whether the path formed by any two visible points intersects the obstacle of the environmental space during the collision avoidance planning process. Therefore, this paper adopts the method based on relative position detection for discrimination, as shown in figure 5, that is, to determine whether the line segment $P1P2$ composed of path point $P1$ and path point $P2$ intersects the polygon obstacle $ABCDE$ .

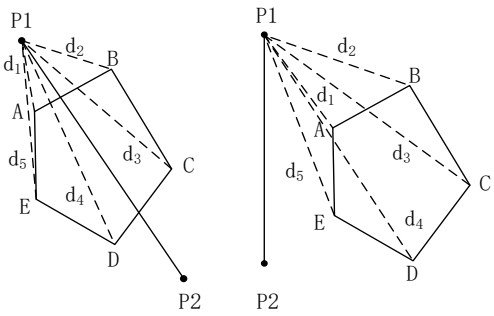


FIGURE 5. Method based on relative position detection

The method based on relative position detection is to firstly figure out the distance $d_1$ , $d_2$ , $d_3$ , $d_4$ and $d_5$ between the endpoint $P1$ and each vertex of the obstacle. And it sorts them according to the distance size to select the two obstacle vertices closest to the starting point $P1$ of the path. Then it judges whether the boundary line of the obstacle with the two vertices closest to $P1$ as the endpoints intersects. As shown in figure 5, it is determined whether $P1P2$ intersects $AE$ , $AB$ and $BC$ . If they intersect, $P1P2$ will conflict with obstacles. Therefore, the question of whether path $P1P2$ intersects with obstacles in environmental space turns into the question of whether $P1P2$ intersects $AE$ , $AB$ and $BC$ .

This article has been accepted for publication in a future issue of this journal, but has not been fully edited. Content may change prior to final publication. Citation information: DOI 10.1109/ACCESS.2019.2907783, IEEE Access



Where Line segment $P1P2$, $AE$, $AB$ and $BC$ can be expressed by line formula (5) :

$$Ax+By+C=0 \tag{5}$$

According to the formula of the distance from point (x,y) to straight line, the distance $d_a$ and $d_b$ from point $A$ and $B$ to path segment $P1P2$ and the distance $d_{P1}$ and $d_{P2}$ from point $P1$ and $P2$ to $AB$ are calculated respectively, as shown in formula (6). Where the distance is signed plus or minus.

$$d=\left(Ax+By+C\right)/\sqrt{A^2+B^2} \tag{6}$$

As shown in figure 5, if the point is above the line segment, the distance $d$ from the point to the line segment is less than zero. If the point is below the line segment, $d$ of the line segment is greater than zero. According to the above rules, the distance from point $A$ and $B$ to path segment $P1P2$ is $d_a$ and $d_b$. If $d_a \times d_b < 0$ and $d_{P1} \times d_{P2} < 0$, the boundary line $AB$ of the obstacle intersects path $P1P2$. If $d_a \times d_b < 0$ and $d_{P1} \times d_{P2} \geq 0$, $AB$ and $P1P2$ do not intersect. If $d_a$ and $d_b$ are not equal to zero at the same time, it means that $AB$ and $P1P2$ only intersect at one vertex $A$ or $B$, and the obstacle has been expanded at this time, so $AB$ and $P1P2$ could be considered as disjoint. If $d_a$ and $d_b$ are equal to zero at the same time, it means that the boundary line $AB$ of the obstacle is on the same line as the path $P1P2$, so $AB$ and $P1P2$ do not intersect. Similarly, whether path $P1P2$ intersects $AE$ and $BC$ could be determined, so as to determine whether path $P1P2$ conflicts with this obstacle.

### B. DYNAMIC ENVIRONMENT MODEL

#### 1) USV ENCOUNTER SITUATIONAL DIVISION

When USV and the target ship can be within the scope of "mutual visibility", the encounter situation of USV can be divided into three situations of encounter, cross encounter and chasing based on COLREGS [30], as shown in figure 6.

- encounter: When the target ship is located within a sector of $355°\sim5°$ centered on the USV.
- cross encounter: When the target ship is located within a sector of $5°\sim112.5°$ centered on the USV, it is called the starboard crossing. When the target ship is located within a sector of $247.5°\sim355°$ centered on the USV, it is called the port side crossing.
- chasing: Take the USV as the overtaking ship, when the USV is located in the sector of $112.5°\sim247.5°$ with the target ship as the center.

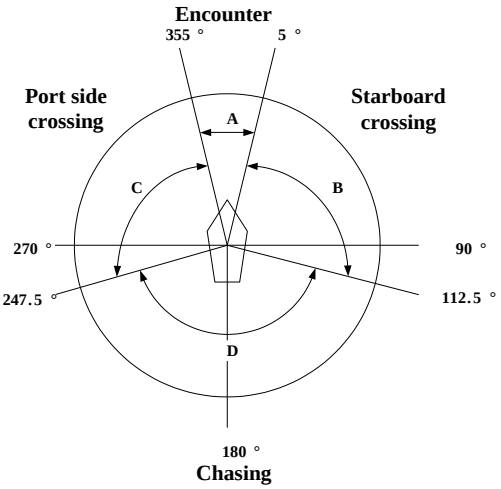


FIGURE 6. USV encounter situational division

Figure 7 shows four situations in which USV encounter collision avoidance based on COLREGS, namely, encounter, chasing, port side crossing and starboard crossing. Where the arrow direction represents the course of the dynamic obstacle, USV finds the dynamic obstacle in "Start", and "Goal" is the USV navigation target point.

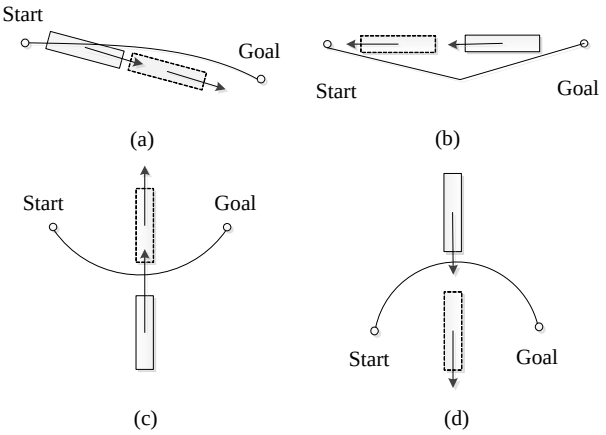


FIGURE 7. (a)Encounter, (b)Chasing, (c)Port side crossing, (d)Startboard crossing

#### 2) USV COLLISION RISK MODEL

In view of the high speed and safety of USV movement, this paper adopts the method of combining fuzzy mathematics and neural network [31] to calculate the risk of collision.

a. membership function of the shortest encounter distance (DCPA):

$$u_{dT}=\begin{cases}1 & |DCPA|<d_1 \\ \frac{1}{2}-\frac{1}{2}\sin\left[\frac{\pi}{d_2-d_1}\cdot\frac{|DCPA|(d_1+d_2)}{2}\right] & d_1<|DCPA|\leq d_2 \\ 0 & d_2<|DCPA|\end{cases} \tag{7}$$

Where $d_1$ is the safe distance for collision avoidance at the latest, $d_2$ is a threshold.

b. membership function of the time (TCPA) that reaches the shortest meeting point:

This article has been accepted for publication in a future issue of this journal, but has not been fully edited. Content may change prior to final publication. Citation information: DOI 10.1109/ACCESS.2019.2907783, IEEE Access



If $TCPA > 0$

$$u_{tT} = \begin{cases} 1 & TCPA \le t_1 \\ \left(\dfrac{t_2 - TCPA}{t_2 - t_1}\right)^2 & t_1 < TCPA \le t_2 \\ 0 & TCPA > t_2 \end{cases} \tag{8}$$

Else

$$u_{tT} = \begin{cases} 1 & TCPA \le t_1 \\ \left(\dfrac{t_2 + TCPA}{t_2 - t_1}\right)^2 & t_1 < TCPA \le t_2 \\ 0 & TCPA > t_2 \end{cases} \tag{9}$$

Where $t_1 = \dfrac{\sqrt{d_1^2 - DCPA^2}}{\Delta v}$, $t_2 = \dfrac{\sqrt{d_2^2 - DCPA^2}}{\Delta v}$.

### 3) DYNAMIC OBSTACLE AVOIDANCE MODEL BASED ON COLREGS

The dynamic obstacle reverse eccentricity expansion method designed in this paper based on COLREGS, that is, the dynamic obstacle provided by AIS system will be reversed eccentricity expansion to the collision avoidance direction required by COLREGS, so that the dynamic obstacle avoidance direction of USV conforms to the COLREGS. As shown in figure 8, where $O^*$ is the reverse eccentric expansion circle, $O'$ is the safety expansion circle, and $R$ is the radius of the dynamic obstacle envelope circle.

a. USV composite collision risk $u_{dt}$:

$$u_{dt} = \min\left(\frac{u_{dT} + u_{tT}}{2}, 1\right) \tag{10}$$

b. reverse eccentric expansion of circle radius $R^*$:

$$R^* = 3R'\left(1 + \frac{2}{3}\sin\left(\frac{\pi}{2}\left(u_{dt} + 2\right)\right)\right) \tag{11}$$

When $u_{dt}$ is small, the dynamic obstacle reverse eccentricity expansion is large, and the impact of collision prevention rules is large. When $u_{dt}$ is large, the dynamic obstacle reverse eccentricity expansion is small, and the impact of collision prevention rules is small.

c. the center of circle $O^*$ is expanded by reverse eccentricity:

$$\begin{cases} O^*(x) = O'(x) + \left(R^* - R'\right)\cos\zeta \\ O^*(y) = O'(y) + \left(R^* - R'\right)\sin\zeta \end{cases} \tag{12}$$

$$\zeta = \begin{cases} \psi + \pi/2, & if \ \text{Encounter} \\ \psi + \pi/2, & if \ \text{Chasing} \\ \psi \pm \pi/2, & if \ \text{Crossing} \end{cases} \tag{13}$$

Where, $\zeta$ is the eccentricity angle of the reverse eccentricity expanded circle. When $\Delta v$ turns to $v_O$ along the arc, if the turn is counterclockwise, it is the left intersection and "±" is +. The opposite is the right cross case, where "±" is −.

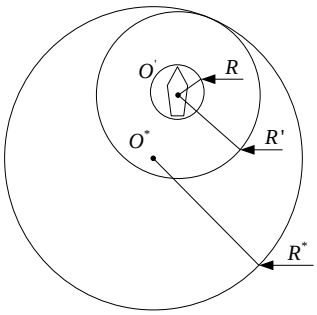


**FIGURE 8. Reverse eccentric puffing effect diagram**

### 4) USV COLLISION AVOIDANCE PLANNING STRATEGY

The motion velocity model of USV and dynamic obstacle is shown in figure 9. In the figure, the boat-borne coordinate system is established with USV as the center. The dynamic obstacle is the reverse eccentrically expanded circle $O^*$. $T$ is the tangent point of circle $O^*$. The USV velocity is $v_{USV}$. The dynamic obstacle velocity is $v_O$ and the relative velocity is $\Delta v$.

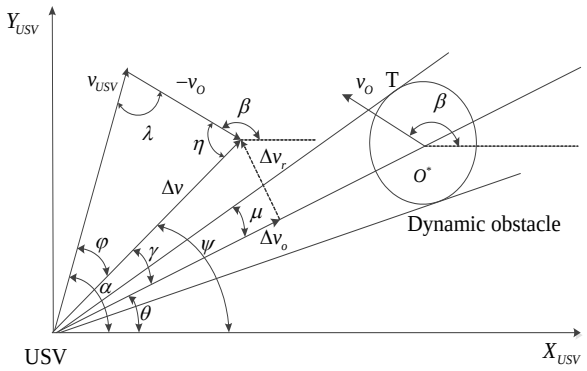


**FIGURE 9. USV and dynamic obstacle motion speed model**

As shown in figure 9, only $abs(\gamma) \ge \mu$ is required to ensure that USV does not collide with dynamic obstacles at any time. $\gamma$ is the included angle between $\Delta v$ and $USV - O^*$ directions. The geometric relationship in the figure can be obtained as $\gamma$:

$$\gamma = \tan^{-1}\frac{v_{USV}\sin(\alpha - \theta) - v_O\sin(\beta - \theta)}{v_{USV}\cos(\alpha - \theta) - v_O\cos(\beta - \theta)} \tag{14}$$

Take the derivative of $\gamma$ and simplify to get:

$$\Delta\gamma = \frac{\sin\varphi}{\Delta v}\Delta v_{USV} + \frac{v_{USV}\cos\varphi}{\Delta v}\Delta\alpha \tag{15}$$

Real-time Angle adjustment $\gamma$ enables USV to meet dynamic collision avoidance condition $|\gamma + \Delta\gamma| \ge \mu$, namely:

$$\begin{cases} \Delta\gamma \ge \mu - r, & if \quad \gamma > 0 \\ \Delta\gamma \le -(\mu + r), & if \quad \gamma < 0 \end{cases} \tag{16}$$

Therefore, according to the dynamic obstacle information provided by the AIS system, reverse eccentric swelling is used to generate virtual obstacle. At this time, USV makes instantaneous static processing for all environmental information, that is, virtual obstacle is regarded as the static known obstacle after instantaneous expansion, and the improved ant colony optimization algorithm designed in this

This article has been accepted for publication in a future issue of this journal, but has not been fully edited. Content may change prior to final publication. Citation information: DOI 10.1109/ACCESS.2019.2907783, IEEE Access



paper can be used to plan a real-time safe air route at this moment. Moreover, based on the motion velocity model of USV and dynamic obstacle, the optimal $\Delta v_{USV}$ and $\Delta\alpha$ should be solved simultaneously to meet the dynamic collision avoidance condition of USV for avoiding dynamic obstacle. Therefore, USV collision avoidance planning in a known dynamic environment can be regarded as a multi-condition objective optimization problem in a known instantaneous static environment, as shown in the following formula.

$$\begin{cases} f(\Delta v_{USV},\Delta\alpha)=\min\left(m_1\left|\Delta v_{USV}\right|+m_2\left|\Delta\alpha\right|\right) \\ \dfrac{\sin\varphi}{\Delta v}\Delta v_{USV}+\dfrac{v_{USV}\cos\varphi}{\Delta v}\Delta\alpha\ge\mu-r, \quad if\ \ \gamma>0 \\ \dfrac{\sin\varphi}{\Delta v}\Delta v_{USV}+\dfrac{v_{USV}\cos\varphi}{\Delta v}\Delta\alpha\le-(\mu+r), \quad if\ \ \gamma<0 \end{cases} \tag{17}$$

Where $f(\Delta v_{USV},\Delta\alpha)$ is the objective optimization function of IACO, and $m_1$ and $m_2$ are the weights of $\Delta v_{USV}$ and $\Delta\alpha$ respectively.

## III. IMPROVED ANT COLONY OPTIMIZATION ALGORITHM

### A. STATE TRANSITION RULES BASED ON DIRECTION ANGLE WEIGHTS

In the USV workspace model, the angle between the ant origin and terminal line and the positive east direction is defined as the course angle $\omega$. While the angle between the ant real-time position and terminal line and the positive east direction is defined as the real-time course angle $\omega_e$, so the real-time course $F_q$:

$$F_q=\frac{\omega_e\cdot\omega}{\left\|\omega_e\right\|\cdot\left\|\omega\right\|} \tag{18}$$

State transition rules refers to the ant to choose the next state point $S$ criterion, this paper uses the pseudo-random proportion rule implementation based on real-time heading angle state transition, by adding the weights of direction angle this coefficient, can choose the path optimization of ants, increase the convergence speed of ACO, the state transition probability design as shown below:

$$s=\begin{cases} \arg\max_{j\in allowed_k}\left\{\left[\tau_{ij}(t)\right]^{\alpha}\cdot\left[\eta_{ij}(t)\right]^{\beta}\cdot\dfrac{1}{F_q}\right\} & if\ \ q\le q_0 \\ S & else \end{cases} \tag{19}$$

$$p_{ij}^{k}(t)=\begin{cases} \dfrac{\left[\tau_{ij}(t)\right]^{\alpha}\left[\eta_{ij}(t)\right]^{\beta}}{\sum_{r\in allowed_k}\left[\tau_{ir}(t)\right]^{\alpha}\left[\eta_{ir}(t)\right]^{\beta}}\cdot\dfrac{1}{F_q} & if\ \ j\in allowed_k \\ 0 & else \end{cases} \tag{20}$$

Where $\tau$ is the pheromone concentration function, $allowed_k$ is the set of viewable points of point $k$ that ant $i$ is allowed to make state transition, $\eta$ is the heuristic function, $\alpha$ is the importance of pheromone, $\beta$ is the importance of the heuristic function.

### B. GLOBAL PHEROMONE UPDATE MODEL BASED ON WOLF GROUP ALLOCATION PRINCIPLE

In order to avoid the local optimum and improve the convergence speed, this paper uses the wolf pack allocation principle to update the pheromone globally. Because the wolves will eliminate the thin wolves based on the natural law of survival of the fittest, leaving a strong wolf to ensure the success of foraging and improve the survival of the wolves. Therefore, this paper uses the principle of wolf pack allocation for reference to conduct pheromone enhancement on the path traveled by the top quartile of ants in each generation:

$$\tau_{ij}(t+n)=(1-\alpha)\tau_{ij}(t)+\Delta\tau_{ij}(t) \tag{21}$$

$$\Delta\tau_{ij}(t)=\begin{cases} \dfrac{Q}{L_{BEST}} & if\ \ (i,j)\text{belongs to the global optimal path} \\ 0 & else \end{cases} \tag{22}$$

Where $\alpha$ is the global pheromone volatility coefficient, $L_{BEST}$ is the length of the current global optimal path.

$$\begin{aligned} \tau_{ij}(t+1)&=\lambda\times\tau_{ij}(t+n) \\ \lambda&=1+0.5\times\frac{D}{L_k} \end{aligned} \tag{23}$$

Where $D$ is the euclidean distance from the starting point to the end point.

### C. MMAS-BASED GLOBAL PHEROMONE UPDATE MODEL

In order to make the optimization algorithm still have certain exploration ability in the later stage of search, this paper uses MMAS for reference and limits the pheromone processing after the completion of the global pheromone update based on the wolf pack allocation principle:

$$\tau_{ij}(t+1)=\begin{cases} \tau_{\min} & if\ \ \tau_{ij}(t+1)<\tau_{\min} \\ \tau_{\max} & if\ \ \tau_{ij}(t+1)>\tau_{\max} \\ \tau_{ij}(t+1) & else \end{cases} \tag{24}$$

Where $\tau_{\min}$ and $\tau_{\max}$ are the upper and lower limits of their own pheromone concentration.

## IV. SIMULATION RESULTS AND ANALYSIS

### A. USV COLLISION AVOIDANCE PLANNING SIMULATION RESULTS IN STATIC UNKNOWN ENVIRONMENT

In order to verify the effectiveness of the USV collision avoidance planning method based on IACO, ACO and IACO have been simulated and compared based on Qt.

According to the environment model of USV, each parameter is set to: $\alpha=1$, $\beta=7$, $\rho=0.3$, $Q=300$, $m=30$, $N_{\max}=500$. And the USV has a speed of 50 knots. In order to verify the superiority of IACO, the global environment has been taken as a rolling window and ACO and IACO have been run repeatedly. The optimal path and algorithm average iteration by the two optimization algorithms are shown in figure 10, 11 and table 1.

This article has been accepted for publication in a future issue of this journal, but has not been fully edited. Content may change prior to final publication. Citation information: DOI 10.1109/ACCESS.2019.2907783, IEEE Access



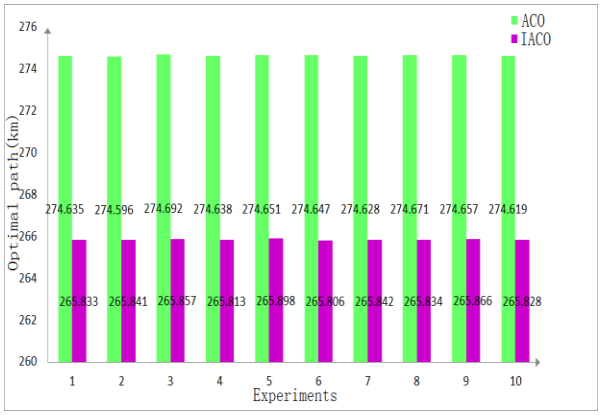


FIGURE 10. Multi-test USV optimal path comparison

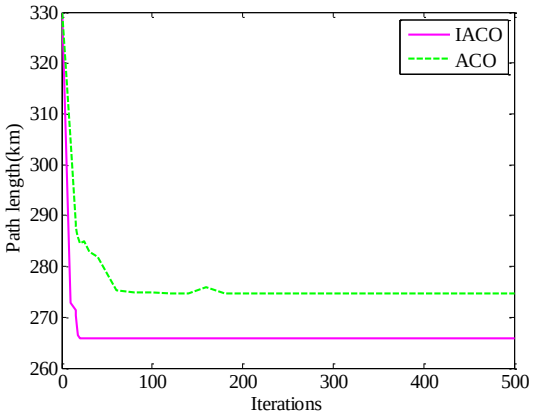


FIGURE 11. Multi-test algorithm average iteration curve

TABLE I
MULTI-TEST COMPARISONS OF ACO AND IACO

| Algorithms | Optimal length(km) | Average iterations | Average times(ms) |
|---|---|---|---|
| ACO | 274.6 | 50 | 957 |
| IACO | 265.8 | 20 | 306 |

By comparing the optimal path length, heading and heading difference of the two ACOs in figure 11-13, it can be intuitively seen that the path of ACO is relatively long and the heading changes greatly when USV sails. While the path of IACO is relatively short and the heading changes little. Based on the data analysis in figure 10 and table 1, it can be seen that:

- the optimal path length of ACO is greater than IACO. ACO of the optimal average path length is about 274.6 km, while IACO is about 265.8 km and relatively stable, this suggests that the optimal path from IACO is better than ACO.
- In terms of the average number of iterations, the number of iterations below 275 km is basically greater than 50 by ACO. And the average time of ACO is 957 ms. Those show that ACO has a slow search speed, and the optimization algorithm is prone to premature stagnation, so it is easy to fall into local optimal. However, IACO can basically plan the path length below 266 km after 20 iterations, and the average time of IACO is 306 ms, indicating that IACO has strong search ability and fast convergence speed.

The collision avoidance planning process of ACO and IACO are shown in figure 14, where the green and purple solid lines respectively represent the planning results of ACO and IACO. It can be seen from the figure that the path smoothness and efficiency planned by IACO are better.

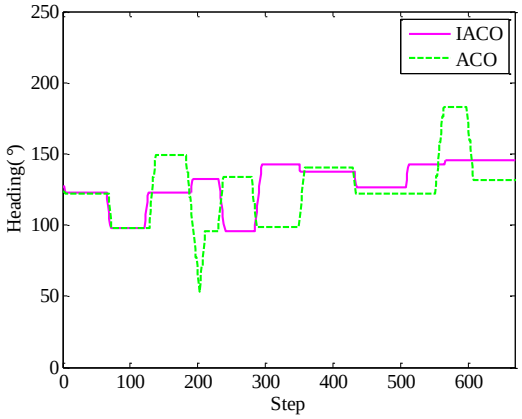


FIGURE 12. USV heading change comparison

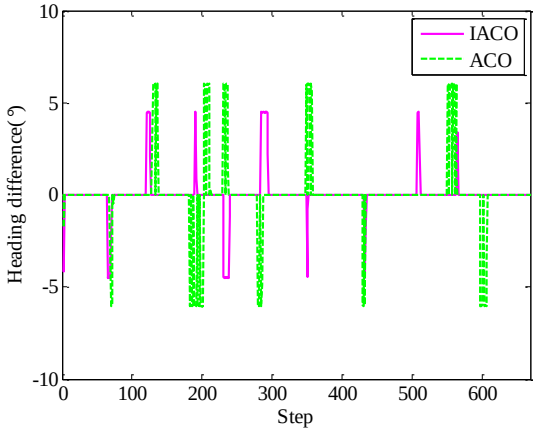


FIGURE 13. Heading difference change comparison

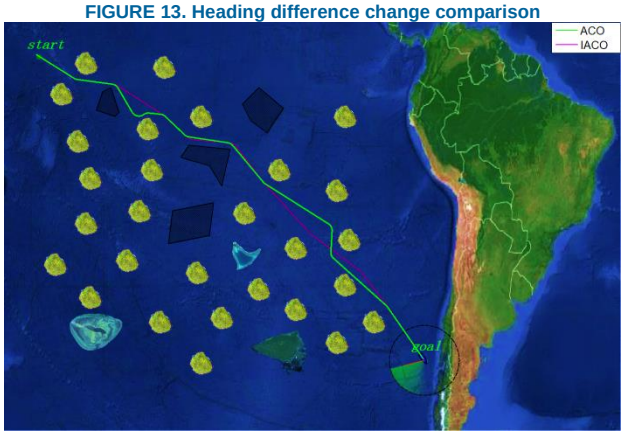


(a)

This article has been accepted for publication in a future issue of this journal, but has not been fully edited. Content may change prior to final publication. Citation information: DOI 10.1109/ACCESS.2019.2907783, IEEE Access



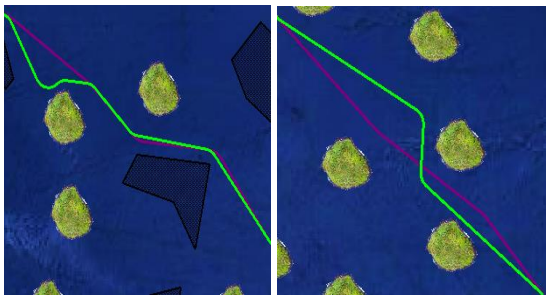

(b) (c)

**FIGURE 14. (a)Overall comparison chart USV, (b)Magnification chart 1, (c)Magnification chart 2 of collision avoidance planning comparison chart**

The results show that ACO has weak searching ability, poor searching ability and effect. IACO has strong search ability, fast convergence speed and high efficiency. In addition, IACO has good experimental results in solving concave polygon obstacles and local optimization.

### *B. SIMULATION RESULTS OF USV COLLISION AVOIDANCE PLANNING FOR DYNAMICALLY KNOWN ENVIRONMENTS*

Based on Qt, the collision avoidance planning of the known dynamic environment based on COLREGS is firstly divided into four kinds of encounter situations for simulation verification: encounter, chasing, port side crossing and startboard crossing, as shown in figure 15. Where USV cruising speed $v_{USV} = 40kn$ , maximum speed $v_{USV\max} = 60kn$ , and dynamic obstacle speed $v_O = 20kn$ .

As can be seen from figure 15~19, by establishing a motion velocity model, the USV takes the reverse eccentrically expanded circle of the dynamic obstacle as the collision avoidance area. In the collision avoidance process, the safety of the USV and the dynamic obstacle is not only guaranteed, but also the avoidance direction of the USV conforms COLREGS. Since the USV finds the collision risk in the first place and the USV is far away from the dynamic obstacle at this time, so USV has enough time to combine with COLREGS to dynamically avoid collision. Therefore, USV only realizes collision avoidance planning by adjusting the course in the case of encounter, port side crossing and startboard crossing. In the case of chasing, the course and speed are adjusted at the same time. The highest speed of USV is adopted to surpass the dynamic obstacle, and the cruise speed of USV is restored after collision avoidance.

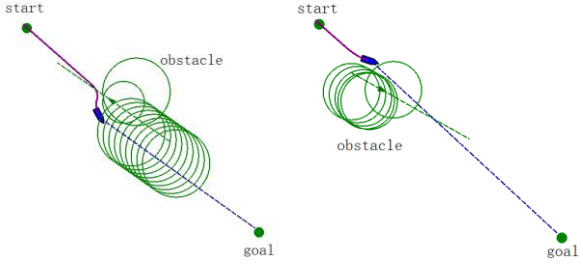


(a) (b)

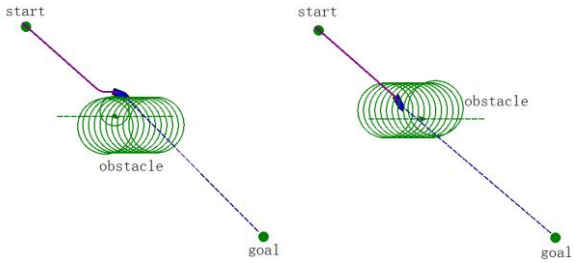


(c) (d)

**FIGURE 15. (a)Encounter, (b)Chasing, (c)Port side crossing, (d)Startboard crossing of USV collision avoidance planning based on COLREGS**

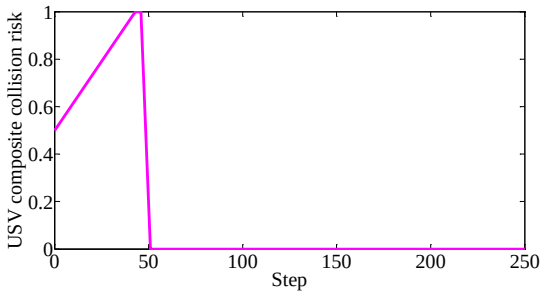


**FIGURE 16. Composite collision risk of USV encounter based on collision avoidance rules**

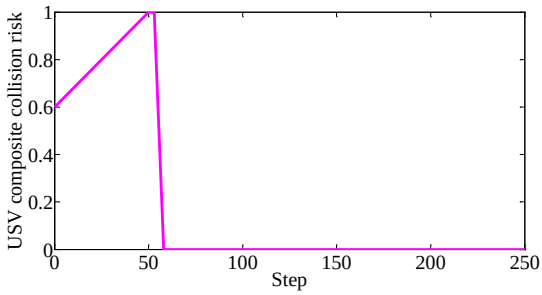


**FIGURE 17. Composite collision risk of USV chasing based on collision avoidance rules**

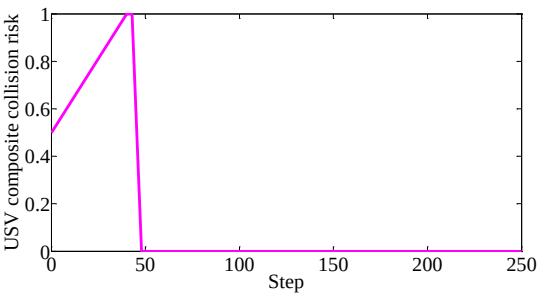


**FIGURE 18. Composite collision risk of USV port side crossing based on collision avoidance rules**

This article has been accepted for publication in a future issue of this journal, but has not been fully edited. Content may change prior to final publication. Citation information: DOI 10.1109/ACCESS.2019.2907783, IEEE Access



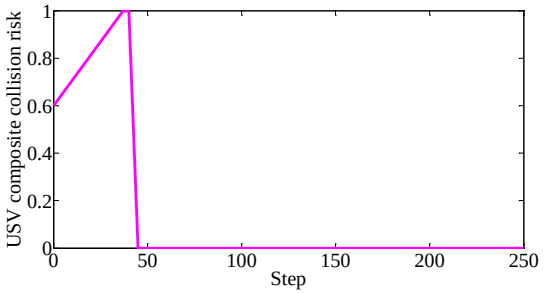


**FIGURE 19. Composite collision risk of USV startboard crossing based on collision avoidance rules**

Secondly, this paper simulates and verifies the collision avoidance planning of multiple dynamic known obstacles based on COLREGS, as shown in figure 20.Where USV cruising speed $v_{USV} = 40kn$, maximum speed $v_{USV\max} = 60kn$, dynamic encountering obstacle 1 speed $v_{O1} = 20kn$, dynamic overtaking obstacle 2 speed $v_{O2} = 20kn$, dynamic left crossing obstacle 3 speed $v_{O3} = 50kn$. In order to make the route of collision avoidance planning clearer, the reverse eccentrically expanded circle of dynamic obstacle is not shown in the simulation.

In figure 20, USV firstly avoids the encountering obstacle 1 only by adjusting the course. Secondly, the course and speed are adjusted simultaneously to avoid the overtaking obstacle 2, and the highest speed of USV is adopted to surpass the obstacle 2 until the collision avoidance is realized. Then the cruise speed of USV is restored. Due to the fast speed of the left intersection obstacle 3, it is difficult for USV to achieve collision avoidance according to its cruising speed. So at this time USV adopts deceleration strategy to complete collision avoidance planning while adjusting the course. Finally, USV first returns to its cruising speed for a period of time until it is not far away from the end point. And it slows down to the end point by itself.

In addition, figure 21~23 show the heading, heading difference and velocity change curve of USV multi-dynamic known obstacle collision avoidance planning based on COLREGS. It can be seen from the figure that the track planned by USV is relatively smooth, and the adjustment process of heading, heading difference and velocity all meet the constraint conditions of USV collision avoidance planning under the condition of high-speed movement.

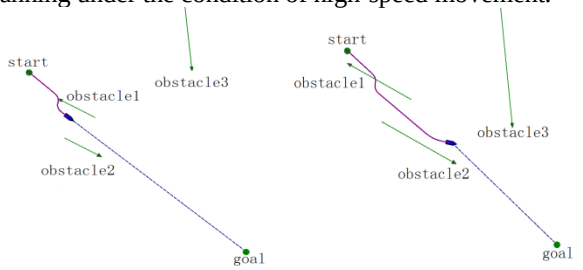


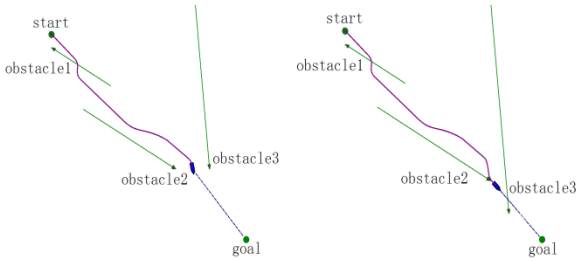


**FIGURE 20. Simulation of multi - dynamic known obstacle avoidance planning for USV based on COLREGS**

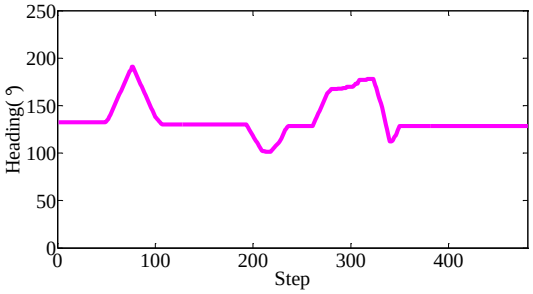


**FIGURE 21. USV heading change curve**

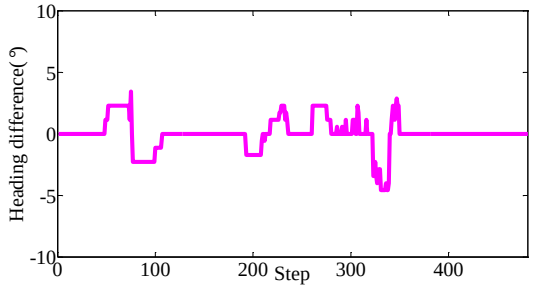


**FIGURE 22. USV heading difference change curve**

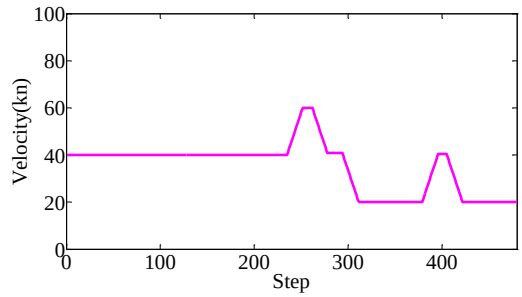


**FIGURE 23. USV velocity change curve**

The analysis results show that according to the known dynamic obstacle information provided by AIS, the dynamic collision avoidance planning of USV based on directional eccentric expansion and motion speed model can not only realize the safe collision avoidance of USV, but also make the avoidance direction of USV conform to COLREGS.

## V. CONCLUSION

Based on the analysis of the disadvantages of ant colony optimization algorithm in USV collision avoidance planning, such as insufficient search ability, slow convergence speed and be easy to fall into local optimum, aiming at the static unknown environment, this paper has combined the dynamic

environment modeling method with IACO to improve the capability of local dynamic programming of USV, and proposed a viewable method to construct the environment model. Based on the motion velocity model and COLREGS, a reverse eccentric expansion method for dynamic obstacles has been designed. In addition, the improved pseudo-random proportion rule has been adopted to select ant state transition, which greatly has improved the convergence speed of ant colony optimization algorithm. Based on the principle of wolf pack allocation and MMAS, the pheromone has been updated globally, which not only has avoid the interference of pheromone on the worst path, but also has avoid the search getting trapped into local optimum. Finally, USV collision avoidance planning in static unknown environment and dynamic known environment has been realized by IACO. Simulation results show that the proposed approach is feasible and effective. In addition, this method has been specially combined with the actual motion characteristics of USV to avoid the danger caused by large and frequent heading adjustment to the high-speed navigation of USV, which is of certain practical significance to the research on safe navigation control of USV.

## REFERENCES

[1] H. Mousazadeh, H. Jafarbiglu, H. Abdolmaleki, et al. "Developing a navigation, guidance and obstacle avoidance algorithm for an unmanned surface vehicle (USV) by algorithms fusion," *Ocean Engineering*, vol. 159, no. 6, pp. 56-65, Jul. 2018, 10.1016/j.oceaneng.2018.04.018.

[2] S. Campbell, W. Naeem, G. W. Irwin. "A review on improving the autonomy of unmanned surface vehicles through intelligent collision avoidance manoeuvres," *Annual Reviews in Control*, vol. 36, no. 2, pp. 267-283, Dec. 2012, 10.1016/j.arcontrol.2012.09.008.

[3] R. J. Yan, S. Pang, H. B. Sun, et al. "Development and missions of unmanned surface vehicle," *Journal of Marine Science and Application*, vol. 09, no. 4, pp. 451-457, Dec. 2010, 10.1007/s11804-010-1033-2.

[4] C. C. Kao, C. M. Lin, J. G. Juang, "Application of potential field method and optimal path planning to mobile robot control," in *Proc. CASE*, Gothenburg, Sweden, 2015, pp. 1552-1554.

[5] P. Svec, M. Schwartz, A. Thakur, et al. "Trajectory planning with look-ahead for unmanned sea surface vehicles to handle environmental disturbances," in *Proc. IROS*, San Francisco, CA, USA, 2011, pp. 1154-1159.

[6] Y. Liu, R. Buknall. "Path planning algorithm for unmanned surface vehicle formations in a practical maritime environment," *Ocean Engineering*, vol. 97, no. 3, pp. 126-144, Mar. 2015, 10.1016/j.oceaneng.2015.01.008.

[7] H. Kim, D. Kim, J. U. Shin, et al. "Angular rate-constrained path planning algorithm for unmanned surface vehicles," *Ocean Engineering*, vol. 84, no. 6, pp. 37-44, Jul. 2014, 10.1016/j.oceaneng.2014.03.034.

[8] C. K. Tam, R. Bucknall. "Collision risk assessment for ships," *Journal of Marine Science & Technology*, vol. 15, no. 3, pp. 257-270, Sep. 2010, 10.1007/s00773-010-0089-7.

[9] C. K. Tam, R. Bucknall. "Path-planning algorithm for ships in close-range encounters," *Journal of Marine Science & Technology*, vol. 15, no. 4, pp. 395-407, Dec. 2010, 10.1007/s00773-010-0094-x

[10] R, Song, Y. Liu, R. Bucknall. "A multi-layered fast marching method for unmanned surface vehicle path planning in a time-variant maritime environment," *Ocean Engineering*, vol. 129, no. 1, pp. 301-317, Jan. 2017, 10.1016/j.oceaneng.2016.11.009.

[11] C. H. Song. "Global path planning method for USV system based on improved ant colony algorithm," *Applied Mechanics and Materials*, vol. 568-570, no. 2014, pp. 785-788, Jun. 2014, 10.4028/www.scientific.net/AMM.568-570.785.

[12] X. Chen, Y. Y. Kong, X. Fang, Q. D. Wu, "A fast two-stage ACO algorithm for robotic path planning," *Neural Computing and Applications*, vol. 22, no. 2, pp. 313-319, Feb. 2013, 10.1007/s00521-011-0682-7.

[13] C. T. Yen, M. F. Cheng. "A study of fuzzy control with ant colony algorithm used in mobile robot for shortest path planning and obstacle avoidance," *Microsystem Technologies*, vol. 24, no. 1, pp. 125-135, Jan. 2018, 10.1007/s00542-016-3192-9.

[14] Y. Xun, M. Liu, Z. Yuan, et al. "Ant colony based on cat swarm optimization and application in picking robot path planning," in *Proc. ICSESS*, Beijing, China, 2017, pp. 162-165.

[15] Z. Yuan, H. Yu, M. Huang. "Improved ant colony optimization algorithm for intelligent vehicle path planning," in *Proc. ICIICII*, Wuhan, China, 2018, pp. 6738-6743.

[16] Y. Gan, F. T. Qu, F. J. Sun, et al. "Research on path planning for mobile robot based on ACO," in *Proc. CCDC*, Chongqing, China, 2017, pp. 1-4.

[17] P. Joshy, P. Supriya. "Implementation of robotic path planning using ant colony optimization algorithm," in *Proc. ICICT*, Coimbatore, India, 2016, pp. 1-6.

[18] R. Rashid, N. Perumal, I. Elamvazuthi, et al. "Mobile robot path planning using ant colony optimization," in *Proc. ROMA*, Ipoh, Malaysia, 2016, pp. 1-6.

[19] L. Jie, Q. D. Yan, M. A. Yue, et al. "Global path planning based on improved ant colony optimization algorithm for geometry," *Journal of Northeastern University*, vol. 36, no. 7, pp. 923-928, Jul. 2015, 10.3969/j.issn.1005-3026.2015.07.003.

[20] T. Stutzle, H. Hoos. "MAX-MIN ant system and local search for the traveling salesman problem," in *Proc. ICEC'97*, Indianapolis, IN, USA 1997, pp. 309-314.

[21] Y. Yao, Q. Ni, L. V. Qing. "A novel heterogeneous feature ant colony optimization and its application on robot path planning," in *Proc. CEC*, Sendai, Japan, 2015, pp. 522-528.

[22] U. Cekmez, M. Ozsiginan, O. K. Sahingoz, "A UAV path planning with parallel ACO algorithm on CUDA platform," in *Proc. ICUAS*, Orlando, FL, USA, 2014, pp. 347-354.

[23] I. Chaari, A. Koubaa, S. Trigui, "Smartpath: An efficient hybrid aco-ga algorithm for solving the global path planning problem of mobile robots," *International Journal of Advanced Robotic Systems*, vol. 11, no.7, Jan. 2014, 10.5772/58543.

[24] J. Cao, "Robot global path planning based on an improved ant colony algorithm," *Journal of Computer and Communications*, vol. 4, no. 2, pp. 11-19, Feb. 2016, 10.4236/jcc.2016.42002..

[25] Y. Zhang, Z. Liu, C. Le. "A new adaptive artificial potential field and rolling window method for mobile robot path planning," in *Proc. CCDC*, Chongqing, China, 2017, pp. 7144-7148.

[26] M. Zimmermannn, C. König. "Integration of a visibility graph based path planning method in the ACT/FHS rotorcraft," *Ceas Aeronautical Journal*, vol. 7, no.3, Sep. 2016, 10.1007/s13272-016-0197-0.

[27] W. U. Hu-Sheng, F. M. Zhang, W. U. Lu-Shan. "New swarm intelligence algorithm——wolf pack algorithm," *Systems Engineering & Electronics*, vol. 35, no.11, pp. 2430-2438, Nov. 2013, 10.3969/j.issn.1001-506X.2013.11.33.

[28] L. Taizhi, Z. Chunxia, X. Pingping. "Global path planning based on simultaneous visibility graph construction and A~* algorithm," *Journal of Nanjing University of Science & Technology*, vol. 41, no. 3, pp. 313-321, Mar. 2017, 10.14177/j.cnki.32-1397n.2017.41.03.007.

[29] J. Cao, Y. Li, S. Zhao, et al. "Genetic-Algorithm-Based Global Path Planning for AUV," in *Proc. ISCID*, Hangzhou, China, 2017, pp. 79-82.

[30] S. Campbell, W. Naeem. "A Rule-based Heuristic Method for COLREGs-compliant Collision Avoidance for an Unmanned Surface Vehicle," *IFAC Proceedings Volumes*, vol. 45, no. 27, pp. 386-391, Sep. 2012, 10.3182/20120919-3-IT-2046.00066.

[31] S. Chen, R. Ahmad, B. G. Lee, et al. Composition ship collision risk based on fuzzy theory, *Journal of Central South University*, vol. 21, no. 11, pp. 4296-4302, Nov. 2014, 10.1007/s11771-014-2428-z.